Available online at www.sciencedirect.com
ScienceDirect
Biochimie 89 (2007) 301–310
BIOCHIMIE
www.elsevier.com/locate/biochi

A 40.7 kDa Rpp30/Rpp1 homologue is a protein subunit of *Dictyostelium discoideum* RNase P holoenzyme

Anastassios Vourekas [a], Dimitra Kalavrizioti [a], Ioannis K. Zarkadis [b], Georgios A. Spyroulias [c], Constantinos Stathopoulos [d,**], Denis Drainas [a,*]

[a] *Department of Biochemistry, School of Medicine, University of Patras, Greece*
[b] *Department of Biology, School of Medicine, University of Patras, Patras 265 04, Greece*
[c] *Department of Pharmacy, University of Patras, Patras 265 04, Greece*
[d] *Department of Biochemistry and Biotechnology, University of Thessaly, Larissa 412 21, Greece*

Received 19 October 2006; accepted 24 November 2006
Available online 30 November 2006

Abstract

RNase P is an essential and ubiquitous endonuclease that mediates the maturation of the 5′ ends of all precursor tRNA molecules. The holoenzyme from *Dictyostelium discoideum* possesses RNA and protein subunits essential for activity, but the exact composition of the ribonucleoprotein complex is still under investigation. Bioinformatic analysis of *D. discoideum* genome identified seven open reading frames encoding candidate RNase P protein subunits. The gene named *drpp30* encodes a protein with a predicted molecular mass of 40.7 kDa that clusters with Rpp1 and Rpp30 RNase P protein subunits from *Saccharomyces cerevisiae* and human respectively, which have significantly lower molecular masses. Cloning and heterologous expression of DRpp30 followed by immunochemical analysis of RNase P active fractions demonstrates its association with RNase P holoenzyme. Furthermore, we show that DRpp30 can bind *D. discoideum* RNase P RNA and tRNA transcripts *in vitro*, giving a first insight of its possible role in *D. discoideum* RNase P function. Homology modeling using as a template the archaeal Ph1887p, and molecular dynamics simulations of the modeled structure suggest that DRpp30 adopts a TIM-barrel fold.

Keywords: RNase P; DRpp30; tRNA; Ribonucleoprotein; Molecular dynamics simulations

1. Introduction

Ribonuclease P (RNase P) is a ubiquitous and essential endonuclease, responsible for the maturation of the 5′ end of all precursor tRNA transcripts. The RNase P holoenzyme is in almost all cases a ribonucleoprotein complex and has been characterized in organisms representing all three kingdoms of life (Archaea, Bacteria and Eukarya) as well as in mitochondria and chloroplasts [1,2]. The discovery that the RNA subunit from bacteria [3] and recently from some archaea [4] is catalytically active *in vitro* in high ionic strength and in the absence of the protein fraction of RNase P, changed our understanding of biological catalysis and attracted significant research attention. Such activity has yet to be proven for the eukaryotic RNA subunit, but it is still considered to be a ribozyme intrinsically [5]. Contrary to the RNA, the protein complement of different RNase P enzymes displays considerable variation [6]. Bacteria have one small subunit [1], archaea likely have no more than 5 protein subunits [7–11] and some eukaryotes have nine (*Saccharomyces cerevisiae*) [12] or ten protein subunits (human) [13]. Among eukaryotes, the complete protein sets are only known for RNase P holoenzymes

Abbreviations: RNase P, ribonuclease P; DRpp30, *Dictyostelium* RNase P Protein 30; Pre-tRNA, precursor transfer RNA; RNP, ribonucleoprotein; EST, expressed sequence tags; DTT, dithiothreitol; PMSF, phenylmethanesulfonyl fluoride; SDS, sodium dodecyl sulfate; PAGE, polyacrylamide gel electrophoresis.

* Corresponding author. Tel.: +30 261 099 7746; fax: +30 261 099 7690.
** Corresponding author. Tel.: +30 241 056 5278; fax: +30 241 056 5290.
E-mail addresses: cstath@bio.uth.gr (C. Stathopoulos), drainas@med.upatras.gr (D. Drainas).

0300-9084/$ - see front matter © 2006 Elsevier Masson SAS. All rights reserved.
doi:10.1016/j.biochi.2006.11.006

from *S. cerevisiae* and human. The first contains 9 protein subunits (Pop1p, Pop3-Pop8p, Rpp1, Rpr2) with apparent molecular weights ranging from 15.5 to 100 kDa [12]. The human RNase P holoenzyme contains a total of 10 protein subunits (hPop1, hPop5, Rpp40, Rpp38, Rpp30, Rpp29, Rpp25, Rpp21, Rpp20 and Rpp14) ranging from 14 to 115 kDa [13], 6 of them being homologous to *S. cerevisiae* (hPop1/Pop1, Rpp30/Rpp1, Rpp29/Pop4, Rpp21/Rpr2, Rpp20/Pop7p, hPop5/Pop5). Although not characterized yet, genomic analysis reveals a remarkable conservation as well as a notable variation in many other eukaryotic organisms, with homologous genes being present for Pop4/Rpp29, Rpr2/Rpp21, Rpp1/Rpp30 and Pop5/hpop5 [14]. The homologous archaeal counterparts of these four proteins have been shown to be integral parts of RNase P holoenzyme either by immunochemical analysis [7] or by reconstitution assays [8,9]. It is considered that primordial catalytic RNase P RNA acquired these four proteins before the evolutionary separation of the archaeal and eukaryotic lines [15]. Despite the considerable amount of data concerning the protein complements of the various RNase P holoenzymes, little is known about their exact role in the structural stability and function of RNase P. The scientific spotlight has recently turned in that direction, as recent studies provide substantial information toward the understanding of the RNase P proteins' contribution to the structural and functional attributes of the holoenzyme [10,11,16–18].

The low buoyant density (1.23 g/ml) of *Dictyostelium discoideum* RNase P, which is the lowest among the eukaryotic RNase P enzymes characterized so far, attests its high protein content [1,19]. Although it has been established that this enzyme contains both essential RNA and protein components, very little is known about the exact composition of the ribonucleoprotein complex. A recent report identified a putative RNA subunit of *D. discoideum* RNase P with a length of 369 nucleotides based on phylogenetic comparative analysis [20]. However, this RNA subunit has not been tested yet *in vitro* to prove its role. Genomic analysis of the available data from *D. discoideum* sequencing projects, revealed the existence of seven open reading frames homologous to previously characterized RNase P protein subunits from human. The encoded proteins (Pop1, DRpp30, DRpp40, DRpp29, DRpp25, DRpp20, DRpp14) exhibit significant similarity as well as notable variation to all their counterparts from other species characterized so far. Rpp30/Rpp1 proteins participate in the minimal holoenzyme composition [15], and therefore the characterization of this protein in *Dictyostelium* was of particular interest. This report describes our experimental approach to identify the *drpp30* gene, to explore the association of the gene product with the RNase P holoenzyme from *D. discoideum*, and to reveal the first functional and structural characteristics of this protein.

2. Materials and methods

2.1. General

Standard molecular biology techniques were used for cloning, transformation and screening. The *D. discoideum* cDNA lambda ZAPII library was made from RNA extracted from 10 h starved and 45 h migrating slug cells (strain AX4).

2.2. Growth of D. discoideum and partial RNase P purification

Growth of *D. discoideum* cells, cell homogenization, RNase P activity recovery and enzyme assays were essentially carried out as previously described [19]. The purification scheme included two steps of anion exchange chromatography (DEAE 52 cellulose, Whatman) and a final purification step by cesium sulfate density gradient centrifugation of concentrated RNase P sample.

2.3. Molecular cloning of drpp30

Bioinformatic analysis [21] of the EST data base of the cDNA sequencing project (http://www.csm.biol.tsukuba.ac.jp/cDNA project.html) resulted in two partially overlapping cDNA clones (CFA817 and VFO634), which are included in Contig-U14170-1 and contain one open reading frame displaying similarity to human Rpp30, and was named *drpp30* (*Dictyostelium R*Nase *P* protein 30). A 266-base pair fragment of *drpp30* (*Δdrpp30*) was amplified from a lambda ZAPII cDNA library (a gift from Dr. Dan Fuller) using the primers 5′-ACTGCATAT GAGTACAAGTAGTGGTTGG-3′ (sense) and 5′-CAGTCTCG AGACATTGTCTAACTCTTTCAGG-3′ (antisense) and was used as a probe for the screening of the cDNA library. The pBluescript SK(−) phagemid containing the *drpp30* open reading frame (ORF) was prepared by *in vivo* excision with helper phage R408 and both DNA strands were sequenced. Sequencing data revealed that 51 bp of the 3′ end of the gene were missing from the isolated clone. Based on the genomic DNA sequencing data which were released while this work was in progress in *dictyBase* (http://www.dictybase.org/), we amplified, cloned and sequenced a 608 bp fragment spanning the *drpp30* ORF stop codon, in order to verify the *drpp30* open reading frame. The complete ORF was cloned by RT–PCR on *D. discoideum* total RNA using two primers positioned on the exact 5′ and 3′ ends (sense: 5′-GCCATGGTTTACTATGATTTAAATATTG-3′; anti-sense: 5′-CTCGAGTTCCCTTTTTCTTTATTATTATC-3′). The sequence of *drpp30* was deposited in NCBI database (GenBank accession number AY940192).

2.4. Overexpression and purification of recombinant DRpp30

drpp30 was cloned into the pET20b expression vector (Novagen), bearing a C-terminal His_6-tag. The recombinant plasmid was sequenced to ensure that no mutations had taken place and was introduced into *Escherichia coli* BL21(DE3)-pLysS competent cells. DRpp30-His_6 was affinity purified from the soluble protein fraction on a Ni^{2+}-nitriloacetic acid agarose column (Qiagen) followed by a step of anion exchange chromatography (DE-52). SDS–PAGE analysis and silver staining of the gels determined that the preparations

of the recombinant polypeptides were devoid of residual bacterial proteins.

2.5. Preparation of rabbit polyclonal antibodies

Δdrpp30, which encodes a protein with a predicted molecular mass of ~11 kDa containing potent antigenic epitopes, was cloned into the pET29a expression vector (Novagen), bearing a C-terminal His_6-tag. The recombinant polypeptide was affinity purified on a Ni^{2+}-nitriloacetic acid agarose column, from the insoluble protein fraction under denaturing conditions (8 M urea). Two rabbits were immunized by subcutaneous injections of purified ΔDRpp30-His_6 protein. Sera collected 56 days after the initial immunization injection were the richest in polyclonal anti-DRpp30 as measured by an ELISA assay. Total rabbit IgG were purified from sera samples using Proteus Protein A affinity mini spin columns (Pro-Chem).

2.6. Immunoprecipitation assays

Pre- and post-immune sera were incubated with 1:1 suspension of protein A Sepharose (PAS) in IPP500 buffer (10 mM Tris–HCl, pH 8.0, 500 mM NaCl, 0.1% Nonidet P-40, 0.5 mM PMSF). overnight at 4 °C. After the antibodies were bound to PAS the complex was washed with IPP500 and with IPP150 (same as IPP500, except for 150 mM NaCl). Eight Microlitres of partially purified RNase P diluted in 100 μl of RNase P assay buffer (buffer D: 50 mM Tris–HCl pH 7.6, 10 mM NH_4Cl, 5 mM $MgCl_2$) were added to the beads, and incubated in the presence of 10 U RNasin, 1 mM DTT and 0.5 mM PMSF for 2.5 h at 4 °C under rotation. The mixtures were centrifuged, the supernatants were collected, and the pellets were washed three times with IPP150 and three times with buffer D. Both pellets and supernatants were checked for RNase P activity.

2.7. In vitro transcription of the RNase P RNA gene

Although the complete genome of *D. discoideum* was published recently, the RNase P RNA subunit has not been annotated yet. However, the putative *D. discoideum* RNase P RNA was identified by Marquez et al. [20]. The 369 nucleotide sequence was amplified from *D. discoideum* AX4 genomic DNA (a gift from Dr. Dan Fuller) using the following primers: sense: 5′-TAATACGACTCACTATAGGGTATTGGTTTGAA ACCA-3′; antisense: 5′-GTATCAGTTAGAGATTAATCT-3′ located exactly at the 5′ and 3′ end of the gene. The sense primer incorporates the T7 promoter (underlined) directly upstream the gene sequence. The product was gel purified and was verified by nested PCR using a set of two internal primers (sense: 5′-GAGAATAATATGGGAAGGTCTGAG-3′; antisense: 5′-TTTCCCAACCTTTGTCATACTG-3′), which amplify a 182 bp internal fragment of the RNase P RNA gene. The gene transcript was *in vitro* synthesized using the PCR product as template and T7 RNA polymerase, in the presence of [α-^{32}P]GTP and unlabeled ribonucleotides overnight at 30 °C and was subsequently gel purified by denaturing PAGE.

2.8. Mobility shift assay

A ^{32}P-labeled RNase P RNA transcript (0.01 pmol) or precursor tRNA (p*SupS1*) (0.03 pmol) were incubated with highly purified recombinant DRpp30 in 20 μl binding buffer (5 mM $MgCl_2$, 10 mM NH_4Cl, 10 mM Tris–HCl pH 8.0, 5% glycerol, 1 mM DTT) for 30 min at 25 °C, both in the absence or presence of total RNA from yeast and poly(I)·poly(C), which acted as non-specific competitors. Non-labeled competitors were incubated with the polypeptides for 20 min at 25 °C in binding buffer prior to the addition of the ^{32}P-labeled precursor tRNA. All tRNA species were subjected to a renaturation step (5 min incubation at 75 °C, 10 min at room temperature) before the assay. Mature *SupS1* and 5′ flank fragment were gel purified after a large scale RNase P maturation assay. RNA–protein complexes were electrophoretically analyzed on native 6% polyacrylamide gels in 0.35× TBE buffer, 5% glycerol at 4 °C. The gels were dried, and visualized by autoradiography.

2.9. Computational methods

2.9.1. Sequence alignment and homology modeling

Protein sequences were acquired from the NCBI and SWISS/PROT databases. Sequence alignment was performed using ClustalW algorithm (1.83) [22]. The 3D crystal structure of archaeal Ph1877p RNase P protein subunit from *Pyrococcus horikoshii* (PDB code: 1V77) is currently the only available for a Rpp30/Rpp1 homologue and was used as a template for the determination of DRpp30 structure. The process was based on the alignment of the two polypeptides extracted from the multiple alignment presented in Fig. 1. In this, only the first 236 amino acid residues (out of 366 in total) of DRpp30 are aligned with the Ph1877p sequence. As a consequence, the homology model of DRpp30 structure was confined to the aforementioned residues. 20 structures of DRpp30 were generated using MODELER [23] and the model with the lowest energy was selected. This model was further energy minimized using the SANDER routine of AMBER 8.0 software [24].

2.9.2. Molecular dynamics simulations and model analysis

All calculations were performed using the AMBER 8.0 suite of programs and the parm94 force field of Cornell et al. [24,25] with full representation of solvent with the TIP3P water model [26]. All trajectories were analyzed using the PTRAJ program of AMBER. After centering the solute and shifting the solvent molecules into the primary unit cell (i.e. imaging), the trajectories were analyzed based on the mass-weighted root mean square deviation (rmsd) of protein atoms vs. time, with respect to the initial geometry.

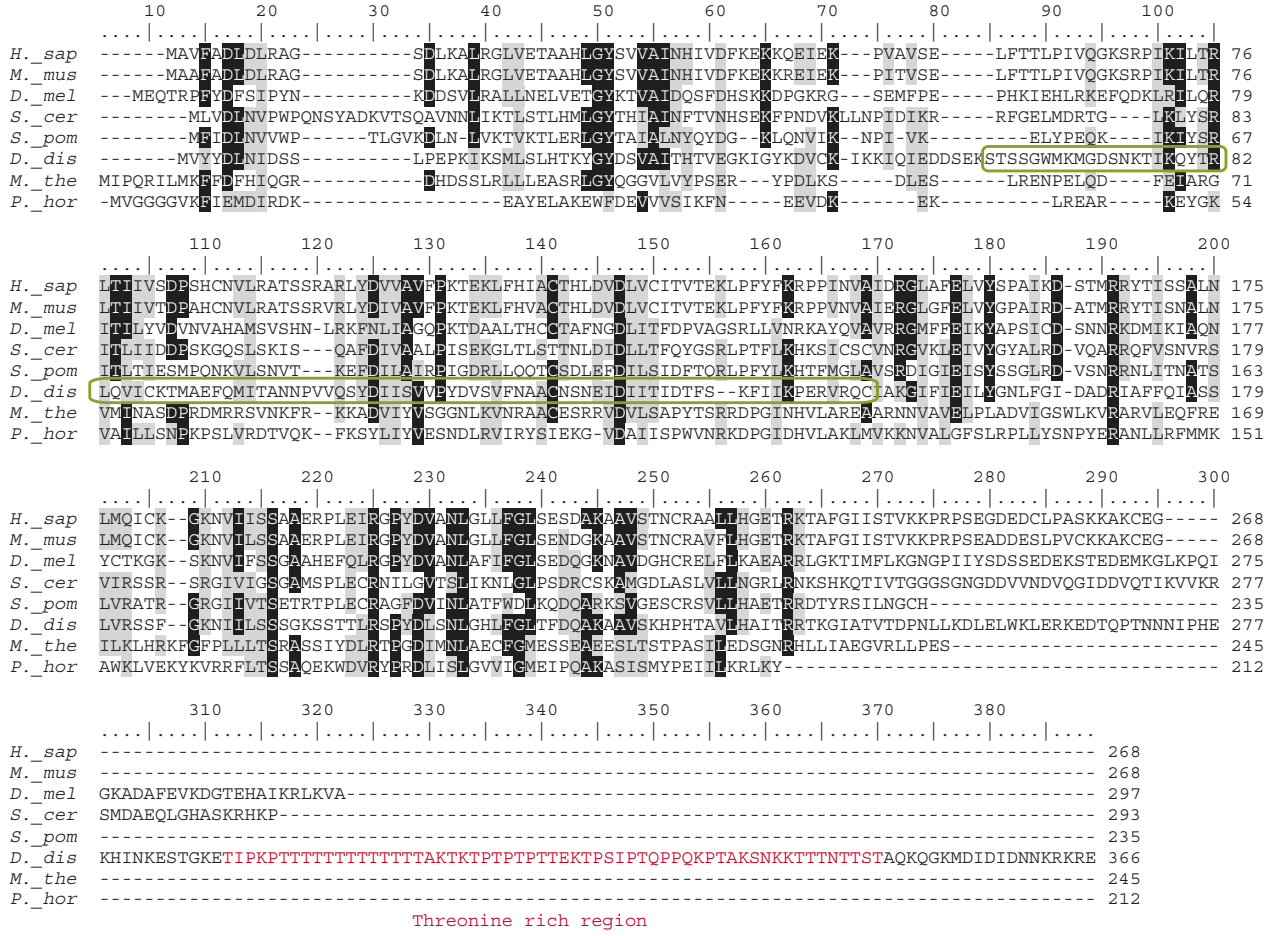

Fig. 1. Multiple sequence alignment of DRpp30 with eukaryotic and archaeal potential homologues. Amino acid sequences were aligned using ClustalW algorithm (1.83) with a slight manual adjustment. Residues exhibiting identity and similarity are highlighted black and gray respectively with a 60% threshold using BLOSUM scoring matrix. Eukaryotic sequences of Rpp30 from *H. sapiens* (*H._sap*, accession no. NP_006404) and Rpp1 from *S. cerevisiae* (*S._cer*, accession no. NP_011929), together with archaeal sequences of Mth688p from *M. thermoautotrophicum* (*M._the*, accession no. F69191) and Ph1877p from *P. horikoshii* (*P._hor*, accession no. H71200) were previously characterized as RNase P protein subunits, whereas sequences from *M. musculus* (*M._mus*, accession no. NP_062301), *S. pombe* (*S._pom*, accession no. P87120), and *D. melanogaster* (*D._mel*, accession no. AAF51526) are predicted, but not experimentally proven to be RNase P subunits. The sequence of ΔDRpp30 is boxed in green. The low complexity region at the C- terminus of DRpp30 is highlighted in red.

3. Results

3.1. Molecular cloning and sequencing of the DRpp30 cDNA clone

Computational search of *D. dictyostelium* cDNA databases (www.csm.biol.tsukuba.ac.jp/cDNAproject.html) using the sequence of Rpp30 [27] revealed an open reading frame (named *drpp30*) that encodes a protein that exhibits significant similarity to previously identified as well as putative RNase P protein subunits (Fig. 1). This high level of similarity suggests the participation of DRpp30 in the formation of *D. discoideum* RNase P holoenzyme. To test this hypothesis, the *drpp30* gene was cloned and overexpressed. A fragment of the gene product that encodes a unique polypeptide with predicted strong antigen epitopes was also cloned and used for the production of antibodies against DRpp30.

The *drpp30* 1101 bp ORF, which corresponds to a gene product of 366 amino acid residues with a predicted molecular mass of 40.7 kDa and a theoretical p*I* of 9.5, was verified by sequence analysis. The primary structure of *drpp30* is identical to the one annotated at *dictyBase* (www.dictybase.org), with the exception of the nucleotide in position 528 (C instead of T). However, this difference does not affect the translated polypeptide sequence (both ATC and ATT triplets code for isoleucine) and more likely represents either a silent genetic polymorphism or a possible sequencing error in the EST sequence.

The amino acid sequence of DRpp30 was aligned using Clustal W algorithm (1.83) [22] with those of *S. cerevisiae* Rpp1 [28], *Homo sapiens* Rpp30 [27], *Methanothermobacter thermoautotrophicum* Mth688p [7], *Pyrococcus horikoshii* Ph1877p [8], and amino acid sequences derived from *Mus musculus*, *Drosophila melanogaster* and *Schizosaccharomyces pombe* ESTs (Fig. 1). The similarity of DRpp30 to human Rpp30 is much higher than to yeast Rpp1 and is primarily located near the C terminus (residues 170–240).

DRpp30 harbors two distinctive structural patterns that were identified using Pfam and Prosite prediction tools [29,30]. Firstly, the RNase P p30 core (residues 80 to 228)

is a characteristic motif of RNase P proteins, possibly required for interaction within the RNase P holoenzyme [31]. In addition, a low complexity region (residues 285 to 347) is located at the carboxy-terminus, rich in threonine and, to a lesser extent, in proline and lysine residues (Fig. 1). Using the above bioinformatic tools we couldn't detect any common RNA binding domain, an observation reported before for other RNase P protein subunits [32,12].

3.2. DRpp30 co-purifies with RNase P active fractions from D. discoideum

The recombinant constructs for *drpp30* were expressed in *E. coli* BL21(DE3)pLysS under various conditions for optimization of protein yield (data not shown). The purified ΔDRpp30-His_6 was used for immunization of rabbits. Pre- and post- immune sera were collected and tested by dot blotting against DRpp30-His_6 and RNase P samples. Post-immune serum was reactive to both samples, whereas pre-immune serum was reactive to none.

D. discoideum RNase P was purified from the S-100 fraction using two steps of anion exchange chromatography and a final step of cesium sulfate density gradient centrifugation. Fractions spanning the peak of enzymatic activity were screened for DRpp30 presence by immunoblotting, using purified rabbit total IgG from post immune serum. As shown in Fig. 2, the polyclonal antiserum recognized a single protein band that coincides exactly with the peak of RNase P activity retrieved from the Cs_2SO_4 density gradient centrifugation. The protein band migrates at an apparent MW of ~41.5 kDa, in good agreement to the calculated MW of DRpp30 (40.7 kDa). Pre-immune serum showed no reactivity when tested under the same conditions.

3.3. Anti-DRpp30 polyclonal antibodies immunoprecipitate RNase P activity

The ability of anti-DRpp30 polyclonal antibodies to recognize DRpp30 in its native context was tested in an attempt to confirm the participation of DRpp30 in the holoenzyme complex of RNase P. IgG coated protein A-Sepharose beads were incubated with partially purified RNase P. The beads were washed under stringent conditions to ensure the specificity of the antigen–antibody interaction responsible for the RNase P activity pull-down and were separated from the supernatants by centrifugation. Post-immune serum coated Sepharose beads effectively precipitated catalytically active RNase P, in contrast to pre-immune serum coated beads (Fig. 3). In addition, a small but considerable depletion of the remaining RNase P activity was observed in the supernatants after treatment with post-immune sera coated beads, in comparison with samples taken after treatment with pre-immune sera coated beads (~20%, reproducibly observed and calculated by Cerenkov counting of the excised gel bands).

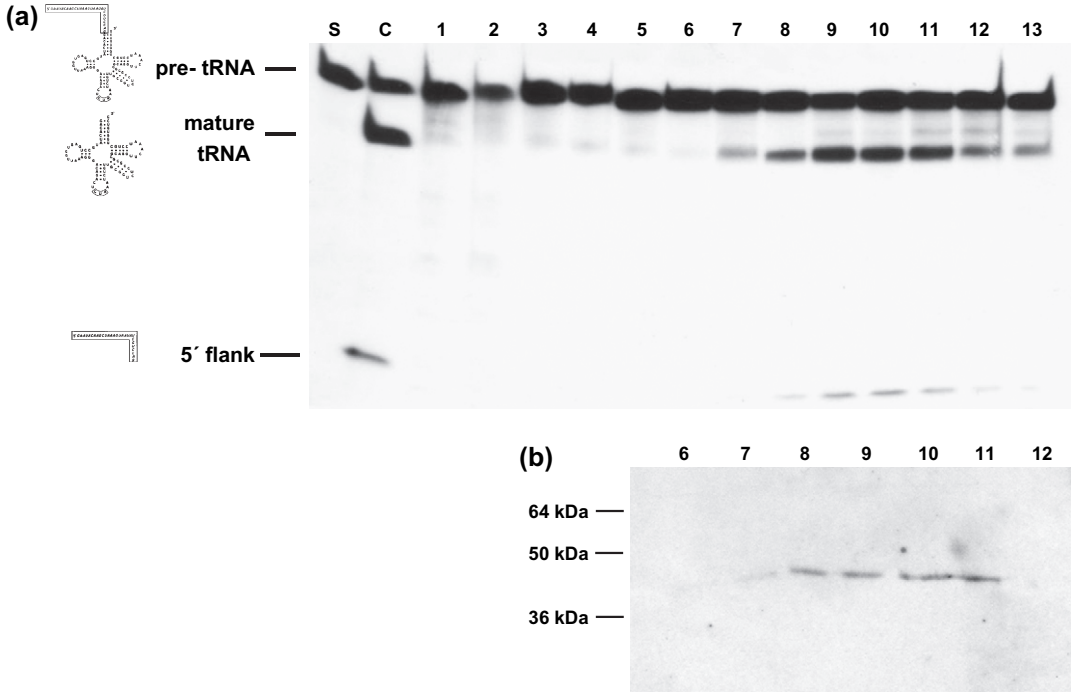

Fig. 2. DRpp30 co-purifies with RNase P activity from *D. discoideum*. (a) Fractions from the final purification step were assayed for RNase P activity using ^{32}P-labeled p*SupS1* as substrate. Reaction products were electrophoretically analyzed on a 10% polyacrylamide/8 M urea gel. S, pre-tRNA substrate alone; C, control RNase P reaction; 1–13, cesium sulfate density centrifugation fractions. RNase P cleaves the p*SupS1* (110 nucleotides), producing the mature tRNA (82 nucleotides) and the 5′ leader sequence (5′ flank, 28 nucleotides). The corresponding bands are marked on the left-hand margin. (b) The same fractions were subjected to western-blot analysis using anti-DRpp30 polyclonal antibodies. DRpp30 was detected only in active fractions. On the left the positions of protein molecular mass markers are indicated.

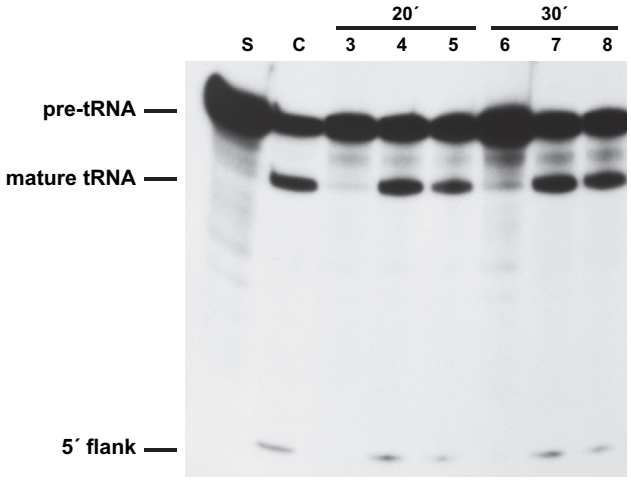

Fig. 3. Immunoprecipitation of RNase P activity with polyclonal antibodies against ΔDRpp30-His_6. Rabbit antiserum was used to immunoprecipitate RNase P activity from a partially purified *D. discoideum* RNase P preparation. Protein A Sepharose beads coated with pre-immune serum (lanes 3 and 6) or serum after immunization with ΔDRpp30-His_6 (lanes 4 and 7: 56 days post immune sera, 5 and 8: 28 days post immune sera) were mixed with partially purified RNase P, washed appropriately and assayed for RNase P activity. Lanes 3, 4, 5 and 6, 7, 8 were incubated for 20 and 30 min, respectively. S, substrate alone; C, control RNase P reaction.

3.4. DRpp30 has RNA binding properties

The archaeal homologue Ph1877p is capable of binding to both the RNase P RNA and pre-tRNA substrate [8,33], while the human homologue, Rpp30, binds RNase P RNA [31] but it was reported not to have pre-*SupS1* binding capacity [17]. Therefore it was interesting to investigate the ability of recombinant DRpp30 protein to interact with both RNase P RNA and (precursor and mature) tRNA. As expected, DRpp30 interacts with the RNase P RNA thus lowering its electrophoretic mobility in 6% native polyacrylamide gels (Fig. 4a, lanes 2–4). More interestingly, DRpp30 forms a stable complex with p*SupS1* (Fig. 4b, lanes 2–4) that appears as a slower migrating band in 6% native PAGE. In some experiments total RNA from yeast and poly(I)·poly(C) were added as non specific competitors. No effects were observed upon addition of up to 500 ng of poly(I)·poly(C) or 100 ng of total yeast RNA (not shown). Total RNA up to 250 and 500 ng moderately affected the formation of the RNA–protein complex, possibly due to tRNA species present in total RNA preparations (Fig. 4b, lane 11 versus lane 4). The DRpp30-p*SupS1* complex is substantially decreased in the presence of increasing concentrations (30- to 90-fold molar excess) of unlabelled p*SupS1*, but the same amounts of mature *SupS1* have a moderate effect on the formation of the complex (Fig. 4b, lanes 8–10 versus 5–7). The interaction of DRpp30 with p*SupS1* was further investigated by oligonucleotide binding interference assays as proposed by Sharin et al. [17]. A short deoxyoligonucleotide (5′-CTGGACGATATTACTTTAGCTTGTATTC-3′) complementary to the 5′ leader sequence of p*SupS1* was allowed to anneal to p*SupS1* during the renaturation step (see Section 2), prior to interacting with DRpp30. With 5 pmol oligonucleotide, the formation of the DRpp30–p*SupS1* complex was completely abolished (Fig. 4b, lane 13). Furthermore, the presence of gel-isolated 5′ leader sequence or a short deoxyoligonucleotide (5′-GAATACAAGCTAAAGTAATATCGTCCAG-3′) identical to the leader sequence in quantities up to 2 pmol (60 molar excess) had no effect on the formation of the complex (not shown).

3.5. DRpp30 folds into a TIM barrel structure

The generation of the DRpp30 homology model was based on the alignment of the DRpp30 amino acid residues 1–235 with residues 7–208 of Ph1877p [33], extracted from the multiple alignment presented in Fig. 1. As a consequence, the homology model of DRpp30 structure was confined to the aforementioned residues. Moreover, the region composed of residues 266–345 has a high propensity for structural disorder, as determined by analysis using the GlobPlot tool [34]. The ribbon diagram of the energy minimized DRpp30 model and the secondary structure elements, as determined using the PROCHECK software [35], aligned with those of Ph1877p, are shown in Fig. 5a and c, respectively. PROCHECK was also used for the analysis of the accuracy of the DRpp30 models. Analysis for the energy minimized homology model, and models extracted every 25 ps for the MD period 500–1000 ps indicates that >98% of the residues backbone φ/ψ dihedral angles are found in favorable regions of the Ramachandran plot. The homology model was then submitted to molecular dynamics simulations. The low rms (root mean square) displacement of the entire model (for backbone and all heavy atoms) and the β-strand core (all atoms) suggests a favorable and stable folding for the modeled DRpp30 structure during the MD course (Fig. 5d).

Homology modeling and molecular dynamics predict that DRpp30 protein folds into an ellipsoid α/β barrel structure bearing seven β-strands and 10 α-helices and one short fragment folded in 3_{10} helix structure (Fig. 5a). DRpp30 and Ph1877p share topological similarities but they also exhibit some differences, such as: (i) the absence of a helix, which in Ph1877p protein is formed between the β2 and β3 strands, probably due to low alignment score between the corresponding DRpp30 and Ph1877p fragments (Fig. 5c), and (ii) the presence of two helical fragments in DRpp30 spanning the residues Glu92-Ser105, namely α2 and α3 helices which are separated by a proline residue (Fig. 5c), while the corresponding region in Ph1877p is folded into a single 12-residue α-helix (namely α3 helix). Therefore, the α/β barrel folding type of DRpp30 models exhibits remarkable topological similarities to the TIM barrel protein structures, as also reported for the Rpp1 protein.

The typical 3D TIM barrel structure consists of eight α-helices positioned at the circumference of a characteristic barrel core formed by eight β strands [36]. The difference between DRpp30 and a typical TIM-barrel structure is that the DRpp30 α10-helix spanning residues Phe218–Ala223 replaces the eighth β-strand segment of a typical TIM barrel structure. The seven stranded DRpp30 barrel core remains

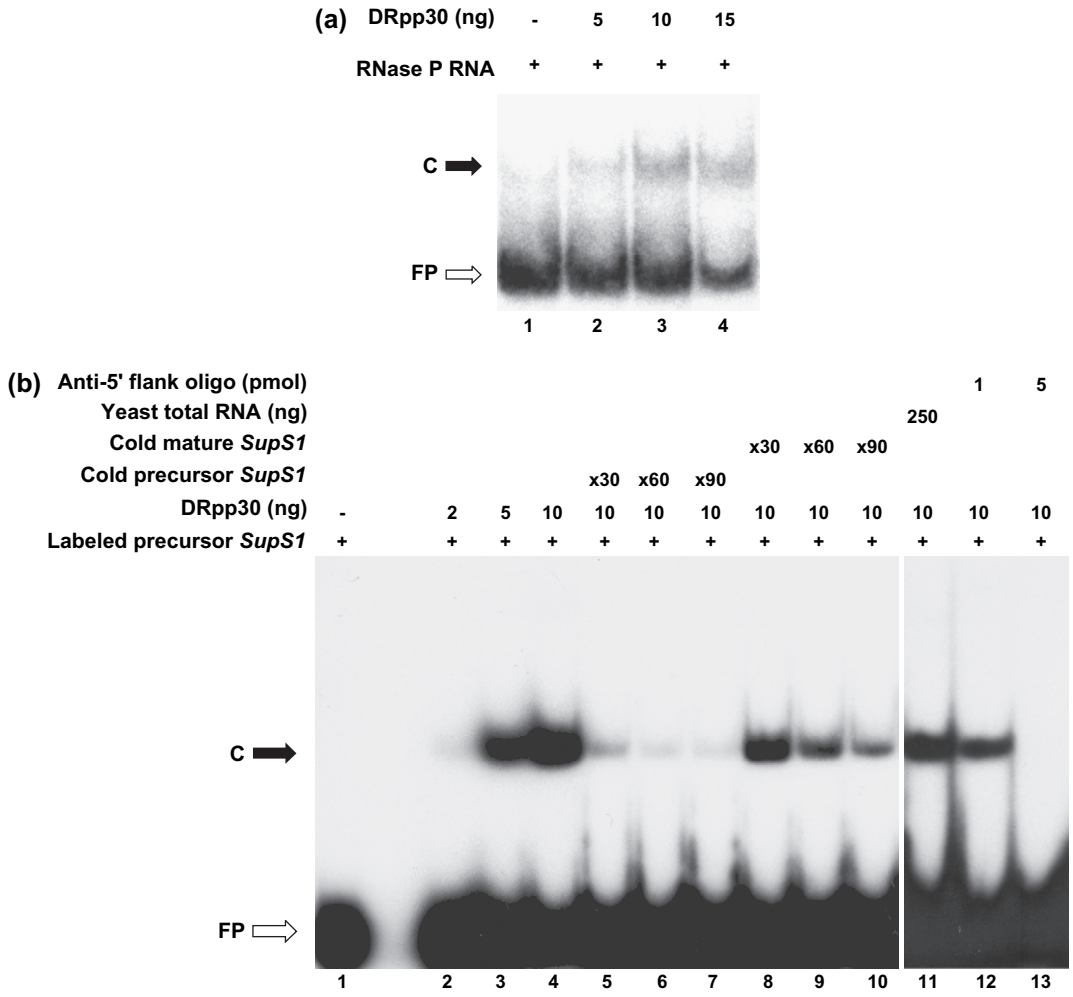

Fig. 4. Electrophoretic mobility shift of RNA species in the presence of DRpp30 polypeptide. The RNA–protein complexes were separated on a 6% native polyacrylamide gel and visualized by autoradiography. The positions of free RNA probe (FP) and protein-RNA complexes (c) are marked by a white and a black arrow, respectively. (a) Internally ^{32}P-labeled RNase P RNA (0.01 pmol) (lane 1) was retarded in the presence of increasing amounts of DRpp30 (lanes 2–4). (b) ^{32}P-labeled p*SupS1* (0.03 pmol) was retarded by DRpp30 and the formation of RNP complexes was tested for competition by specific and non-specific competitors. p*SupS1* (lane 1), was incubated with increasing amounts of DRpp30 (lanes 2, 3, 4). The formation of the RNP complex was considerably inhibited by the presence of increasing concentrations of unlabeled p*SupS1* (30, 60, 90 molar excess; lanes 5, 6, 7). A moderate effect on the complex formation was observed by the presence of the same amounts of mature *SupS1* (lanes 8, 9, 10). Total RNA from yeast did not affect the formation of the complex significantly (lane 11). Increasing amounts of the oligonucleotide complementary to the 5′ leader sequence, substantially inhibited the DRpp30–*pSupS1* interaction (lanes 12 and 13).

remarkably stable as is evidenced by the low rmsd (~1.6–1.7 Å; after the first 40 ps equilibration period) of MD simulations (Fig. 5d). 'Incomplete' barrel consisting of seven strands has been previously reported for the seven-stranded glycosidases (cellulases) (7CEL) [36].

The structure of DRpp30 is characterized by the high density of positive charges of Lys/Arg amine groups, distributed over the molecular surface and the negatively charged β-strand barrel core (Fig. 5b). Numerous basic residues are found at the protein fragment spanning residues 138–152, including the linker between β5 and α5, and α5 helix. Lys152 together with Arg202 and Lys222 are located on the molecule surface pointing towards the solvent. These residues are of special interest since they are found conserved in homologous sequences (Fig. 1) and are thought to play a key role in the interaction of the protein subunit with the RNase P RNA and/or the pre-tRNA substrate of the enzyme [33]. Rms displacement of these residues is relatively low with respect to the initial model, with an average value ~1.5 Å, which indicates that they possess a rather stable conformation/orientation during the MD period.

On the other hand, the negative charge density inside the β-strand barrel is due to highly conserved Asp5 (β1 strand), Asp129 (β5 strand) and Glu157 (β6 strand) and DRpp30 specific Asp9 (β1 strand), and Glu39 (β2 strand) (Fig. 5b).

4. Discussion

We report here on the cDNA cloning, biochemical characterization, and homology modeling of DRpp30 structure. Preliminary cDNA sequencing data available through *Dictyostelium* cDNA project (Tsukuba, Japan) and dictyBase (www.dictybase.org) were used to identify a region in *D. discoideum* chromosome 1 that contains the DRpp30

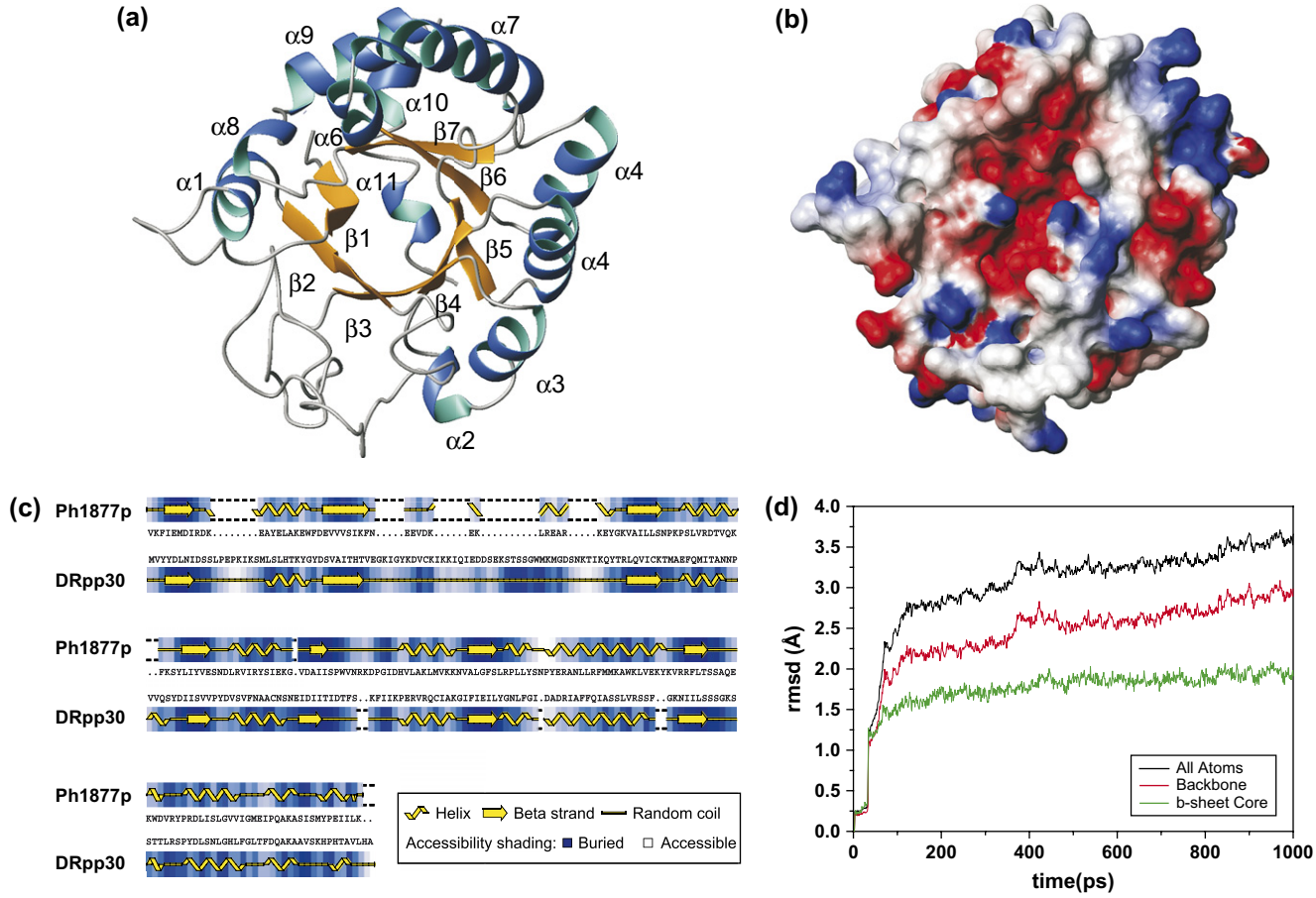

Fig. 5. (a) Homology model of DRpp30. (b) Distribution of electrostatic potentials on the surface of DRpp30 homology model. Red and blue colors indicate negatively and positively charged amino acid residues, respectively. (c) Elements of secondary structure and residue accessibility for DRpp30 and Ph1887p. (d) Rmsd values monitored during the course of 1000 ps MD simulations, for all heavy atoms of DRpp30, for the backbone atoms and for all the atoms comprising the seven β strand core.

open reading frame. The gene named *drpp30* (*Dictyostelium discoideum* RNase P Protein 30) encodes a protein of a predicted molecular mass of 40.7 kDa which exhibits significant similarity to characterized RNase P protein subunits, such as Rpp30 from human [37] (29% identity, 49% similarity at a length of 253 amino acids) and Rpp1 from *Saccharomyces cerevisiae* [28] (22% identity, 43% similarity at a length of 236 amino acids). It must be noted that the molecular masses of the putative DRpp30 homologues range from ∼25 kDa to 33.5 kDa, thus differing significantly in this aspect from their *D. discoideum* counterpart.

DRpp30 is functionally associated with the RNase P ribonucleoprotein catalytic complex. Using anti-DRpp30 antibodies we ascertained the concurrence of DRpp30 with purified RNase P activity after standard purification schemes. Moreover, the nature of this association permits the precipitation of RNase P activity through antigen-antibody interaction using the same antibodies.

Although DRpp30 does not bear any known RNA-binding motifs, it was shown in this study that it can bind both RNase P RNA and tRNA. Interestingly, the archaeal homologue Ph1877p was reported to be capable of binding to both the RNase P RNA and pre-tRNA substrate [8,33], while the human homologue, Rpp30, binds RNase P RNA [31] but shows no pre-*SupS1* binding capacity [17]. The expected DRpp30 interaction with RNase P RNA was confirmed by our results, which are consistent with the above-mentioned data. Whether DRpp30 participates in specific substrate binding was an intriguing question that we explored. DRpp30 interacts with p*SupS1* more strongly than mature *SupS1* as suggested by competition experiments (Fig. 4b, lanes 8–10 versus 5–7). Additionally, a deoxyoligonucleotide that binds to 5′ leader sequence substantially inhibits the formation of the aforementioned complex. Furthermore, gel isolated leader sequence or a deoxyoligonucleotide identical to it failed to inhibit protein binding to the precursor, indicating that this binding is not a result of non-specific single-stranded binding activity. These results indicate that DRpp30 protein shows a preference for binding to the tRNA precursor than to the mature tRNA molecule, and that there is a synergistic contribution of single stranded 5′-leader and mature tRNA body to pre-tRNA binding. This binding could be attributed to the TIM barrel structure that DRpp30 seems to adopt according to MD simulations, as it has been reported for the RNase P protein Ph1877p from *Pyrococcus horikoshii* [33].

DRpp30 contains positively charged residues (pI is 9.5), a characteristic shared by the majority of the known RNase

P protein subunits that most likely allows the protein to interact with negatively charged surfaces, such as the tRNA substrate and/or the RNA subunit of the holoenzyme. A recent report on the *P. horikoshii* RNase P protein subunit Ph1877p (DRpp30 homologue) crystal structure suggests that conserved positively charged amino acid residues (among them are Lys123, Arg176 and Lys196) are important for enzymatic activity of the holoenzyme [33]. According to our Clustal based similarity analysis (Fig. 1), the aforementioned residues are also present in DRpp30 (Lys152, Arg202 and Lys222, respectively). Moreover, as shown by our structural analysis, these residues are positioned at accessible sites on the molecular surface of DRpp30, possibly playing a similar role in *D. discoideum* RNase P holoenzyme. In addition, it has been proposed that highly conserved acidic residues present in yeast Rpp1 protein (Asp4, Asp127 and Glu157) could participate in metal ion coordination (i.e. Mg^{2+}) inside the seven-stranded barrel, that could serve both structural and functional purposes in the RNase P holoenzyme [38]. The same residues are also present in DRpp30 (Asp5, Asp129 and Glu157), further supporting that DRpp30 is homologous to Rpp1. Furthermore, Leu, Ala, Ile and Phe residues contained in helices *α5, α6, α9,* and beta sheets *β6, β7* in all likelihood compose a conserved hydrophobic patch on DRpp30 surface which could facilitate the interaction with other protein partners, as it has been shown for archaeal Rpp30 and Pop5 homologues (an hpop5 homologue exists in *D. discoideum* genome) [10,11].

Despite the overall similarity, DRpp30 stands as a unique protein among its homologues due to the unusual carboxy-terminus that bears a low complexity region (residues 285–347), rich in threonine and to a lesser extent in proline and lysine residues (Fig. 1). GlobPlot tool predicts that this region is unstructured. Disordered regions can contain functional sites, and they are of growing interest, owing to the increasing number of reports of intrinsically unstructured/disordered proteins (IUPs) [34]. This specific region is responsible for the greater mass of DRpp30, compared to its homologues. Although no other known RNase P protein subunit bears such a motif, we noticed that a similar threonine stretch domain exists in the N-terminus of a *Candida albicans* homologue of Rpm1, which was recently identified as a unique RNase MRP protein subunit in yeast [39]. Tandem repeats at the genomic and the protein level are abundant in *D. discoideum* [40], present also in other *D. discoideum* RNase P protein subunits (unpublished data), and it remains to be proven by future mutational analyses whether this feature contributes to the structure and function of these proteins.

As part of an integrative approach, experiments are now in progress to purify soluble forms of various protein subunits of the *D. discoideum* RNase P complex that have been identified through genomic analysis and to investigate their role.

5. Conclusions

D. discoideum RNase P is a ribonucleoprotein consisting of RNA and most probably seven protein subunits. DRpp30 is functionally associated with the RNase P ribonucleoprotein catalytic complex and exhibits significant similarity to characterized RNase P protein subunits, such as Rpp30 from human, Rpp1 from *Saccharomyces cerevisiae* and Ph1877p from *Pyrococcus horikoshii*. Despite the overall similarity, DRpp30 stands as a unique protein among its homologues due to the unusual carboxy-terminus, which harbors a long polythreonine tract. Homology modeling using as a template the archaeal Ph1887p, and molecular dynamics simulations of the modeled structure indicate that DRpp30 adopts a TIM-barrel fold. The structure of DRpp30 is characterized by high density of positive charges distributed around the molecular surface. This feature can explain the RNA binding properties that DRpp30 possesses. Finally, DRpp30 capacity to bind not only RNase P RNA but also tRNA suggests that it might play a central role in RNase P structure and function.

Acknowledgments

We are grateful to Professor Alexios J. Aletras for his help with the production of rabbit antisera. The *D. discoideum* AX4 genomic DNA and cDNA lambda ZAPII library was a kind gift from Dr. Dan Fuller (University of California, San Diego, USA). This work was supported in part by the European Social Fund (ESF), Operational Program for Educational and Vocational Training II (EPEAEK II), Heraklitos.

References

[1] D.N. Frank, N.R. Pace, Ribonuclease P: unity and diversity in a tRNA processing ribozyme, Annu. Rev. Biochem. 67 (1998) 153–180.
[2] S. Xiao, F. Scott, C.A. Fierke, D.R. Engelke, Eukaryotic ribonuclease P: A plurality of ribonucleoprotein enzymes, Annu. Rev. Biochem. 71 (2002) 165–189.
[3] C. Guerrier-Takada, K. Gardiner, T. Marsh, N. Pace, S. Altman, The RNA moiety of ribonuclease P is the catalytic subunit of the enzyme, Cell 35 (1983) 849–857.
[4] J.A. Pannucci, E.S. Haas, T.A. Hall, J.K. Harris, J.W. Brown, RNase P RNAs from some Archaea are catalytically active, Proc. Natl Acad. Sci. U.S.A. 96 (1999) 7803–7808.
[5] D.N. Frank, C. Adamidi, M.A. Ehringer, C. Pitulle, N.R. Pace, Phylogenetic-comparative analysis of the eukaryal ribonuclease P RNA, RNA 6 (2000) 1895–1904.
[6] N.R. Pace, J.W. Brown, Evolutionary perspective on the structure and function of ribonuclease P, a ribozyme, J. Bacteriol. 177 (1995) 1919–1928.
[7] T.A. Hall, J.W. Brown, Archaeal RNase P has multiple protein subunits homologous to eukaryotic nuclear RNase P proteins, RNA 8 (2002) 296–306.
[8] Y. Kouzuma, M. Mizoguchi, H. Takagi, H. Ukuhara, M. Tsukamoto, T. Numata, M. Kimura, Reconstitution of archaeal ribonuclease P from RNA and four protein subunits, Biochem. Biophys. Res. Commun. 306 (2003) 666–673.
[9] W.P. Boomershine, C.A. McElroy, H.Y. Tsai, R.C. Wilson, V. Gopalan, M.P. Foster, Structure of Mth11/Rpp29, an essential protein subunit of archaeal and eukaryotic RNase P, Proc. Natl. Acad. Sci. U.S.A. 26 (2003) 15398–15403.
[10] S. Kawano, T. Nakashima, Y. Kakuta, I. Tanaka, M. Kimura, Crystal Structure of Protein Ph1481p in Complex with Protein Ph1877p of Archaeal RNase P from Pyrococcus horikoshii OT3: Implication of Dimer Formation of the Holoenzyme, J. Mol. Biol. 2 (2006) 583–591.

[11] R.C. Wilson, C.J. Bohlen, M.P. Foster, C.E. Bell, Structure of Pfu Pop5, an archaeal RNase P protein, Proc. Natl. Acad. Sci. U.S.A. 4 (2006) 873–878.
[12] J.R. Chamberlain, Y. Lee, W.S. Lane, D.R. Engelke, Purification and characterization of the nuclear RNase P holoenzyme complex reveals extensive subunit overlap with RNase MRP, Genes Dev. 12 (1998) 1678–1690.
[13] N. Jarrous, Human ribonuclease P: Subunits, function, and intranuclear localization, RNA 8 (2002) 1–7.
[14] E. Hartmann, R.K. Hartmann, The enigma of RNase P evolution, Trends Genet. 19 (2003) 561–569.
[15] D. Evans, S.M. Marquez, N.R. Pace, RNase P: interface of the RNA and protein worlds, Trends Biochem. Sci. 31 (2006) 333–341.
[16] H. Mann, Y. Ben-Asouli, A. Schein, S. Moussa, N. Jarrous, Role of RNA and Protein Subunits of a Primordial Catalytic Ribonucleoprotein in RNA-Based Catalysis, Mol. Cell 12 (2003) 925–935.
[17] E. Sharin, A. Schein, H. Mann, Y. Ben-Asouli, N. Jarrous, RNase P: role of distinct protein cofactors in tRNA substrate recognition and RNA-based catalysis, Nucleic Acids Res. 33 (2005) 5120–5132.
[18] A.H. Buck, A.B. Dalby, A.W. Poole, A.V. Kasantsev, N.R. Pace, Protein activation of a ribozyme: the role of bacterial RNase P protein, EMBO J. 24 (2005) 3360–3368.
[19] C. Stathopoulos, D.L. Kalpaxis, D. Drainas, Partial purification and characterization of RNase P from *Dictyostelium discoideum*, Eur. J. Biochem. 228 (1995) 976–980.
[20] S.M. Marquez, J.K. Harris, S.T. Kelley, J.W. Brown, S.C. Dawson, E.C. Roberts, N.R. Pace, Structural implications of novel diversity in eucaryal RNase P RNA, RNA 11 (2005) 739–751.
[21] S.F. Altschul, T.L. Madden, A.A. Schaffer, J. Zhang, Z. Zhang, W. Miller, D.J. Lipman, Gapped BLAST and PSI BLAST: A new generation of protein database search programs, Nucleic Acids Res. 25 (1997) 3389–3402.
[22] J.D. Thompson, D.G. Higgins, T.J. Gibson, CLUSTAL W: Improving the sensitivity of progressive multiple sequence alignment through sequence weighting, position-specific gap penalties and weight matrix choice, Nucleic Acids Res. 22 (1994) 4673–4680.
[23] N. Eswar, B. John, N. Mirkovic, A. Fiser, V.A. Ilyin, U. Pieper, A.C. Stuart, M.A. Marti-Renom, M.S. Madhusudhan, B. Yerkovich, A. Sali, Tools for comparative protein structure modelling and analysis, Nucleic Acids Res. 31 (2003) 3375–3380.
[24] J. Wang, R.M. Wolf, J.W. Caldwell, P.A. Kollman, D.A. Case, Development and testing of a general amber force field, J. Comput. Chem. 25 (2004) 1157–1174.
[25] W.D. Cornell, P. Cieplak, C.I. Bayly, I.R. Gould, K.M. Merz Jr., D.M. Ferguson, D.C. Spellmeyer, T. Fox, J.W. Caldwell, P.A. Kollman, A second generation force field for the simulation of proteins, nucleic acids, and organic molecules, J. Am. Chem. Soc. 117 (1995) 5179–5197.
[26] W.L. Jorgensen, J. Chandrasekhar, J. Madura, M.L. Klein, Comparison of simple potential functions for simulating liquid water, J. Chem. Phys. 79 (1983) 926–935.
[27] P.S. Eder, R. Kekuda, V. Stolc, S. Altman, Characterization of two scleroderma autoimmune antigens that copurify with human ribonuclease P, Proc. Natl. Acad. Sci. U.S.A. 94 (1997) 1101–1106.
[28] V. Stolc, S. Altman, Rpp1, an essential protein subunit of nuclear RNase P required for processing of precursor tRNA and 35S precursor rRNA in *Saccharomyces cerevisiae*, Genes Dev. 11 (1997) 2926–2937.
[29] A. Bateman, L. Coin, R. Durbin, R.D. Finn, V. Hollich, S. Griffiths-Jones, A. Khanna, S. Moxon, E.L.L. Sonnhammer, D.J. Studholme, et al., The Pfam protein families database, Nucleic Acids Res. 32 (2004) 138–141.
[30] A. Gattiker, E. Gasteiger, A. Bairoch, ScanProsite: a reference implementation of a PROSITE scanning tool, Appl. Bioinformatics 1 (2002) 107–108.
[31] T. Jiang, C. Guerrier-Takada, S. Altman, Protein-RNA interactions in the subunits of human nuclear RNase, P, RNA 7 (2001) 937–941.
[32] C. Guerrier-Takada, P.S. Eder, V. Gopalan, S. Altman, Purification and characterization of Rpp25, an RNA-binding protein subunit of human ribonuclease P, RNA 8 (2002) 290–295.
[33] H. Takagi, M. Watanabe, Y. Kakuta, R. Kamachi, T. Numata, I. Tanaka, M. Kimura, Crystal structure of the Ribonuclease P protein Ph1877p from hyperthermophilic archaeon Pyrococcus horikoshii OT3, Biochem. Biophys. Res. Commun. 319 (2004) 787–794.
[34] R. Linding, R.B. Russell, V. Neduva, T.J. Gibson, GlobPlot: Exploring protein sequences for globularity and disorder, Nucleic Acids Res. 13 (2003) 3701–3708.
[35] R.A. Laskowski, M.W. MacArthur, D.S. Moss, J.M. Thornton, PROCHECK - a program to check the stereochemical quality of protein structures, J. Appl. Crystallogr. 26 (1993) 283–291.
[36] N. Nagano, C.A. Orengo, J.M. Thornton, One fold with many functions: The evolutionary relationships between TIM barrel families based on their sequences, structures and functions, J. Mol. Biol. 321 (2003) 741–765.
[37] N. Jarrous, P.S. Eder, C. Guerrier-Takada, C. Hoog, S. Altman, Autoantigenic properties of some protein subunits of catalytically active complexes of human ribonuclease P, RNA 4 (1998) 407–417.
[38] M. Dlakić, 3D models of yeast RNase P/MRP proteins Rpp1 and Pop3p, RNA 11 (2005) 1–5.
[39] K. Salinas, S. Wierzbicki, L. Zhou, M.E. Schmitt, Characterization and purification of *Saccharomyces cerevisiae* RNase MRP reveals a new unique protein component, J. Biol. Chem. 12 (2005) 11352–11360.
[40] L. Eichinger, et al., The genome of the social amoeba *Dictyostelium discoideum*, Nature 435 (2005) 43–57.